Advances and Applications in Statistics

Published Online: November 2014
Available online at http://pphmj.com/journals/adas.htm
Volume 42, Number 2, 2014, Pages 119-156

STOCHASTIC MODELING OF WAVE EQUATION WITH UNCERTAINTIES IN INITIAL AND BOUNDARY CONDITIONS

Shiang-Jen Wu

National Center for High-Performance Computing
Hsinchu 30076, Taiwan
e-mail: sjwu@nchc.narl.org.tw

Abstract

This study proposes an alternative stochastic modeling framework to quantify the uncertainty propagation of spatiotemporal variables due to variations in initial and boundary conditions by incorporating the explicit numerical solutions of the 1-D wave equation with the expected value operator. Spatiotemporal semivariogram models are employed to deal with the correlation of the variables in time and space. The proposed model is validated by comparing it with the Monte Carlo simulation (MCS) model associated with the explicit numerical solution of the wave equation in the calculation of statistical properties of model outputs, i.e., the mean and coefficient of variance (CV). The results of numerical experiments show that the proposed model can produce excellent approximations of the mean and inferior approximations of the CV as compared to those of the MCS model. Furthermore, by means of the proposed models with varying CV values for the initial and boundary conditions, respectively, we can quantify the resulting effect from conditions based on the estimations of the wave displacement; therefore, it is possible to conclude that

Received: August 6, 2014; Accepted: September 15, 2014
2010 Mathematics Subject Classification: 58J65.
Keywords and phrases: wave equation, Monte Carlo simulation, expected value operator, spatiotemporal semivariogram.

their uncertainties are mainly attributed to the variation of the boundary condition.

1. Introduction

Uncertainty is attributed to the lack of reliable information concerning the phenomena, processes and data involved in problem definition and resolution (Tung and Mays [37]). In general, the degree of uncertainty can be described using statistical moments, such as standard deviation, variance and coefficient of variance (Tung and Yen [38]). The sources of uncertainty are classified as model uncertainty due to assumptions in model equation or building, input uncertainty due to imprecise forecasting, parameter uncertainty due to imperfect assessment and natural operation uncertainty due to unforeseen causes (Maskey [22]). However, there are always some uncertainties related to physical problems, such as those involving: boundary and initial conditions, transport coefficients, sources and interaction terms, geometric irregularities (e.g., roughness) and so on (e.g., Kavvas and Govindaraju [18]; Xiu and Karniadakis [42]; Gottlieb and Xiu [14]; Scharffenberg and Kavvas [33]). These uncertainties can be grouped into three types: random coefficients (e.g., initial condition operators), random right-hand sides (e.g., initial and boundary conditions) and random geometry (boundary shapes) (Gunzburger [15]). Dettinger and Wilson [7] also indicated that uncertainties in numerical models primarily result from spatiotemporal model parameters, boundary/initial conditions and source/sink strength based on the behavior and description of the numerical models of groundwater flow. Hence, the numerical model for estimating spatiotemporal variates should be affected by the uncertainties in the initial and boundary conditions, which are composed of the spatiotemporal variables. That is to say, numerical models governed by the partial differential equations should account for the uncertainties in model parameters, initial and boundary conditions.

Since the spatiotemporal variates belong to random variables, the corresponding governing partial differential equation (PDE) can become the stochastic partial differential equation (SPDE). Hence, the aforementioned

uncertainty in the numerical model can be quantified by solving the SPDE. A number of methods developed to solve the SPDE, involve the perturbation methods through Taylor series (e.g., Collard and Juillard [2]; Lin [21]), the expansion methods through Neumann series (e.g., Yamazaki et al. [44]; Zeitoun and Braester [45]) and the first- and second-order statistical moment method (e.g., Elishakoff et al. [10]; Muscolino et al. [24]; Wang and Hsu [39]). Moreover, some analytical methods for the stochastic structure are implemented by incorporating the stochastic input or parameters into the deterministic model (e.g., Muscolino et al. [24]; Falsone and Impollonia [11]; Impollonia and Ricciardi [17]). Unfortunately, these methods have a number of shortcomings: the limited applicability attributed to restrictive analytical constraints, non-guaranteed convergence of the Taylor as well as Neumann and probable high computation time (DiazDelao and Adhikari [8]). In addition, these methods probably result in obvious error when the variation is relatively large (Muscolino et al. [24]). The Polynomial Chaos (PC) method is also widely used to evaluate uncertainty in a dynamic system attributed to uncertainty in the system parameters (e.g., Xiu and Karniadakis [43]; Nagy and Braatz [25]; Gottlieb and Xiu [14]; Tang and Zhou [36]; Zhou and Tang [46]; Pulch [28, 29]; Agut et al. [1]). However, since the associated chaos expansion converges slowly in a complicated field, the Polynomial Chaos method has generally received little attention for a long time (Xiu and Karniadakis [43]). In summary, an advantage of the Polynomial Chaos method is the exponential convergence with respect to the polynomial order, whereas the disadvantage is the intrusiveness due to the coupled system of equations that has to be solved.

In addition to the aforementioned methods, the Monte Carlo simulation method with the efficient numerical algorithm incorporated is also used to solve general stochastic problems (e.g., Papadrakakis and Papadopoulos [26]; Hurtado and Barbat [16]; Muscolino et al. [24]). It presents a number of advantages: the ability to model a complex system which is superior to an analytical model, decreased system size in regard to the required number of simulating samples and the calculation of statistical moments of outcome, as well as the associated probability distribution (Singh and Kim [34]). In the

framework of the Monte Carlo simulation method, the variables involved in the models and real-life systems should be represented by the probability distribution; thereby, the Monte Carlo simulation method can fully simulate systems many times by choosing a value for each variable based on the suitable probability distributions and on the outcome as a probability distribution of the overall value of the system calculated through the interactions of the model (Kwak and Ingall [19]). Although the Monte Carlo simulation model provides a useful technique for modeling and analyzing a real-life system, it generally requires lengthy computational time to obtain satisfactory statistical moments of model outcomes with poor computational efficiency, especially for a multi-dimensional dynamic system (e.g., Singh and Kim [34]; Su and Strunz [35]; Nagy and Braatz [25]).

Since most phenomena and processes can be described by mathematic models which are mostly governed by the numerical solution of the governing partial differential equations, the corresponding behavior can be described by the numerical solution. In addition, the expected values of the powers of variables are called the *statistical moments of variables*, meaning that the statistical properties of variates can be expressed in terms of the expected values of variables of various powers. The method for using the expected values of variables to calculate the associated statistics is named the expected value operator. Therefore, to effectively analyze uncertainty propagation in a stochastic problem, this study incorporates the expected value operator with the numerical solutions of a candidate model (i.e., the wave equation) to model the approximations of statistical properties, i.e., the mean, standard deviation and coefficient of variance. Since most studies related to stochastic problems focus on the uncertainty in model parameters (e.g., Muscolino et al. [24]; Nagy and Braatz [25]; Gottlieb and Xiu [14]; Tang and Zhou [36]), several investigations indicate that the boundary problem is an important issue in regard to the numerical analysis (e.g., Zhu et al. [47]; Scharffenberg and Kavvas [33]; Pulch [29]); its uncertainty, therefore, should be considered in the numerical computation. The proposed model aims to evaluate the effect of uncertainties in the initial and boundary conditions on the outputs of numerical models.

2. Description of the Proposed Stochastic Modeling Framework

2.1. Basic concept

In general, numerical models are mathematical models that use some sort of numerical time-stepping procedure to derive the behavior of a model over time. The mathematical solution is represented by a numerical solution of the corresponding governing partial differential equation (PDE). Since the analytical solutions of PDEs are derived with difficulty, numerical analysis is frequently carried out to obtain an approximation solution. The numerical solution is arrived at by means of the numerical schemes, such as finite element and different methods. Specifically, the numerical solution of PDEs needs some discretization of the domain into a collection of points or elemental volumes in time and space, so that the numerical solution can be regarded as a function of the unknown spatiotemporal variable at a particular time step and position with respect to the known variables at previous time steps and locations.

The expected value of a random variable is defined as the weighted average of all possible values that this random variable can take on, where each possible value is weighted by its respective probability. The expected value of a random variable X is denoted as $E[X]$, and is often called the *expectation of X* or the *mean of X*. Note that the expected values of the powers of the variables are called the *statistical moments of the variable*, namely, the statistical properties of variables can be obtained by means of the expected value operator as follows:

$$\begin{aligned}
&\text{Mean: } E[X] = \sum x f_y(x) \\
&\text{Variance: } Var[X] = E[X^2] - (E[X])^2 \\
&\text{Standard deviation: } \sigma[X] = \sqrt{Var[X]} \\
&\text{Coefficient of variance: } CV[X] = \sigma[X]/E[X],
\end{aligned} \tag{1}$$

where X stands for the spatiotemporal variate; $E[\bullet]$ and $f_y(\bullet)$ denote the

expected value operator and the probability density function; and $\sigma[X]$ and $Var[X]$ are the standard deviation and variance.

Since the numerical solution serves as the function of variates at various time steps and positions, the proposed stochastic modeling utilizes the expected value operator with the numerical solution of the governing equation incorporated to calculate the statistical properties of model outputs, i.e., the mean, standard deviation and the coefficient of variance, when the statistical moments of initial and boundary conditions are known. Therefore, by means of the proposed model, the uncertainty analysis for the spatiotemporal variates, whose behavior is described by the governing equation, can be carried out by taking into account uncertainties in the boundary and initial conditions.

2.2. Formulation of the expected values using the numerical solution

In general, the numerical solution of the governing equation for a numerical model is derived using the explicit and implicit numerical schemes, such as the finite difference, element and volumes methods. Roberts and Selim [30] indicated that the explicit and implicit schemes have their own advantages and can facilitate the selection of an appropriate numerical scheme with the emphasis placed upon accuracy, computation time and programming effort. In this study, due to the simplification of the formulation of the expected value of the spatiotemporal variable, the numerical solution of the governing equation is derived using the explicit numerical scheme as follows:

$$u_{i+1}^{j+1} = f(u_{i+1}^{j}, u_{i+2}^{j}, u_{i}^{j+1}, ...), \tag{2}$$

where u_{i+1}^{j}, u_{i+2}^{j} and u_{i}^{j+1} denote the spatiotemporal variates at various time steps and positions; and $f(\bullet)$ denotes the explicit numerical solution, namely, the relationship of the variable, u_{i+1}^{j+1}, unknown at the time step $(j+1)$ and position $(i+1)$ with the remaining variates known at previous times and positions.

Since the numerical solution of PDE indicates the relationship of the unknown variate and the known variables, the statistical properties (i.e., the expected values of various orders) of spatiotemporal variates can be calculated by the expected value operator incorporated with the explicit numerical solution. For example, the explicit numerical solution of equation (2) can be illustrated as:

$$u_{i+1}^{j+1} = \theta_1 u_{i+1}^{j} + \theta_2 u_{i+2}^{j} + \theta_3 u_{i+1}^{j-1}, \tag{3}$$

where θ_1, θ_2 and θ_3 are coefficients. Using equation (1), $E[u_{i+1}^{j+1}]$ and $E[(u_{i+1}^{j+1})^2]$ at time step $(j+1)$ and position $(i+1)$ can be obtained by the following equations:

$$E[u_{i+1}^{j+1}] = \theta_1 E[u_{i+1}^{j}] + \theta_2 E[u_{i+2}^{j}] + \theta_3 E[u_{i+1}^{j-1}], \tag{4}$$

$$\begin{aligned} E[(u_{i+1}^{j+1})^2] &= E[(\theta_1 u_{i+1}^{j} + \theta_2 u_{i+2}^{j} + \theta_3 u_{i+1}^{j-1})^2] \\ &= \theta_1^2 E[(u_{i+1}^{j})^2] + \theta_2^2 E[(u_{i+2}^{j})^2] + \theta_3^2 E[(u_{i+1}^{j-1})^2] + 2\theta_1\theta_2 E[u_{i+1}^{j} u_{i+2}^{j}] \\ &\quad + 2\theta_1\theta_3 E[u_{i+1}^{j} u_{i+i}^{j-1}] + 2\theta_2\theta_3 E[u_{i+2}^{j} u_{i+1}^{j-1}]. \end{aligned} \tag{5}$$

The expected value of the spatiotemporal variable calculated by equation (4) accounts for the mean value. The standard deviation and coefficient of variance should be yielded by substituting equations (4) and (5) into equation (2).

2.3. Quantification of the correlation of variables in time and space

In equation (5), since the expected value of the product of two spatiotemporal variables: $E[u_{i+1}^{j} u_{i+2}^{j}]$, $E[u_{i+1}^{j} u_{i+1}^{j-1}]$ and $E[u_{i+2}^{j} u_{i+1}^{j-1}]$ in response to the correlation between the two variables in time and space, should be figured out, this study utilizes the spatiotemporal semivariogram method, which analyzes the covariance matrix of variables in time and space, to calculate the expected value of the product of variables. The spatiotemporal semivariogram model is briefly introduced below.

Since the spatiotemporal semivariogram model can deal with spatially- and temporally-correlated variables (Gneiting et al. [13]), this study adopts the spatiotemporal semivariogram model to quantify the correlation of variable in time and space. The spatiotemporal semivariogram $\gamma_{st}(h_s, h_t)$ is expressed as:

$$\gamma_{st}(h_s, h_t) = \frac{1}{2} Var[Z(x + h_s, t + h_t) - Z(x, t)], \quad (6)$$

where h_s and h_t represent the distance and time lag, respectively; $Z(x, t)$ denotes the spatiotemporal variable at the time *t* and the position *x*. A number of spatiotemporal semivariogram models have been published to describe the behavior of spatiotemporal semivariograms, such as the product of semivariograms (Rodriguez-Iturbe and Mejia [31]), the integrated product of semivariograms (Dimitrakopoulos and Luo [9]), and the product-sum model (De Cesare et al. [5, 6]). Of the above spatiotemporal semivariogram models, the product-sum model has three advantages: (1) it can provide a large class of flexible models that require less constraint symmetry between the spatial and temporal correlation components; (2) it does not need an arbitrary space-time metric; and (3) it can be fitted to data using relatively straightforward techniques, similar to those developed for a spatial-based semivariograms (Gneiting et al. [13]). Accordingly, this study adopts the product-sum method to calculate the spatiotemporal semivariogram of $Z(x, t)$. The concept of the spatiotemporal semivariogram model is briefly introduced below.

The product-sum spatiotemporal semivariogram $\gamma_{st}(h_s, h_t)$ is defined in terms of separate spatial semivariogram $\gamma_s(h_s)$ and temporal semivariogram $\gamma_t(h_t)$ as:

$$r_{st}(h_s, h_t) = r_s(h_s)[k_1 C_t(0) + k_2] + r_t(h_t)[k_1 C_s(0) + k_3] - k_1 C_s(h_s) C_t(h_t), \quad (7)$$

where C_s and C_t are the spatial and temporal covariances, respectively, and $C_s(0)$ and $C_t(0)$ stand for sills, which are defined as the limit values for the semivariograms; they are generally used as parameters in theoretical semivariogram models. Table 1 shows the theoretical semivariogram models

commonly used. k_1, k_2 and k_3 are coefficients and can be computed by using the following equations (De Cesare et al. [5, 6]):

$$k_1 = \frac{C_s(0) + C_t(0) - C_{st}(0, 0)}{C_s(0)C_t(0)},$$

$$k_2 = \frac{C_{st}(0, 0) + C_t(0)}{C_s(0)},$$

$$k_3 = \frac{C_{st}(0, 0) - C_s(0)}{C_t(0)}, \tag{8}$$

where $C_{st}(0, 0)$ denotes the sill of the spatiotemporal semivariogram and, generally, is adopted as the maximum of $C_s(0)$ and $C_t(0)$. In addition to the semivariogram, the covariance and correlation measure the similarity between two different variables; their relationship is shown as:

$$\rho(h_t, h_s) = 1 - \frac{\gamma_{st}(h_t, h_s)}{C_{st}(0, 0)}, \tag{9}$$

where $\rho(h_t, h_s)$ denotes the correlation coefficient of spatiotemporal variables; and $C_{st}(0, 0)$ is a covariance for h_t and h_s being zero, whereby it is equal to the maximum of $C_s(0)$ and $C_t(0)$. The correlation coefficient $\rho(h_t, h_s)$ can be expressed as:

$$\rho(h_t, h_s) = \frac{E\{[Z(x, t) - E(Z(x, t))][Z(x + h_s, t + h_t) - E(Z(x + h_s, t + h_t))]\}}{\sqrt{Var[Z(x, t)]Var[Z(x + h_s, t + h_t)]}},$$

$$Var[Z(x, t)] = E[(Z(x, t))^2] - (E[Z(x, t)])^2,$$

$$Var[Z(x + h_s, t + h_t)] = E[(Z(x + h_s, t + h_t))^2] - (E[Z(x + h_s, t + h_t)])^2. \tag{10}$$

Therefore, by extending equation (10), the expected value of the product of two spatiotemporal variates can be obtained by the following equation:

$$E[Z(x + h_s, t + h_t)Z(x, t)] = E[Z(x, t)]E[Z(x + h_s, t + h_t)]$$
$$+ \rho(h_t, h_s)\sqrt{(Var[Z(x, t)])(Var[x + h_s, t + h_t])}. \tag{11}$$

Accordingly, the expected value of the product of two spatiotemporal variables $E[u_{i+1}^{j}u_{i+2}^{j}]$, $E[u_{i+1}^{j}u_{i+1}^{j-1}]$ and $E[u_{i+2}^{j}u_{i+1}^{j-1}]$ can be obtained using equation (11) as:

$$E[u_{i+1}^{j}u_{i+2}^{j}] = E[u_{i+1}^{j}]E[u_{i+2}^{j}] + \rho(0,\ \Delta x)\sqrt{(Var[u_{i+1}^{j}])(Var[u_{i+2}^{j}])},$$

$$E[u_{i+1}^{j}u_{i+1}^{j-1}] = E[u_{i+1}^{j}]E[u_{i+1}^{j-1}] + \rho(\Delta t,\ 0)\sqrt{(Var[u_{i+1}^{j}])(Var[u_{i+1}^{j-1}])},$$

$$E[u_{i+2}^{j}u_{i+1}^{j-1}] = E[u_{i+2}^{j}]E[u_{i+1}^{j-1}] + \rho(\Delta t,\ \Delta x)\sqrt{(Var[u_{i+2}^{j}])(Var[u_{i+1}^{j-1}])}, \quad (12)$$

where Δt and Δx stand for the time step and distance increment. And $\rho(0,\ \Delta x)$, $\rho(\Delta t,\ 0)$ and $\rho(\Delta t,\ \Delta x)$ can be calculated using equation (12) as:

$$\rho(0,\ \Delta x) = 1 - \frac{\gamma_{st}(0,\ \Delta x)}{C_{st}(0,\ 0)},$$

$$\rho(\Delta t,\ 0) = 1 - \frac{\gamma_{st}(\Delta t,\ 0)}{C_{st}(0,\ 0)},$$

$$\rho(\Delta t,\ \Delta x) = 1 - \frac{\gamma_{st}(\Delta t,\ \Delta x)}{C_{st}(0,\ 0)} \quad (13)$$

in which $\gamma_{st}(0,\ \Delta x)$, $\gamma_{st}(\Delta t,\ 0)$, $\gamma_{st}(\Delta t,\ \Delta x)$ and $C_{st}(0,\ 0)$ can be calculated by equation (7). Eventually, the uncertainty of the spatiotemporal variates estimated by the governing equation due to the variation in the boundary and initial conditions can be evaluated. It should be also pointed out that the formula for calculating the expected value of equations (4) and (5) can serve as the numerical solutions for $E[u_{i+1}^{j-1}]$ and $E[(u_{i+1}^{j+1})^2]$. As a result, programming the proposed model can be completed using common computer coding methods to find the explicit numerical solution of the governing equation. Note that in this study, the selection of the best-fit semivariogram model is conducted by the genetic algorithm based on the parameter sensitivity (GA_SA method) developed by Wu et al. [41]. In the GA_SA method, the parameters of all models are calibrated in association with a minimum value of the objective function in which the root mean square error (RMSE) is commonly used as:

$$RMSE = \left[\frac{1}{NX} \sum_{ix=1}^{NX} (\gamma_{\exp}(ix) - \gamma_{the}(ix))^2 \right]^{1/2}, \quad (14)$$

where $\gamma_{\exp}$ and γ_{the} stand for the semivariogram estimated by data and theoretical model, respectively.

3. Stochastic Modeling of Wave Equation

To demonstrate the applicability of the proposed framework for modeling uncertainty analysis by incorporating the explicit numerical solution of governing equations of numerical models with the expected value operator, this study follows Gottlieb and Xiu's [14] investigation, which analyzed the effect of the parameter (wave velocity) in the one-dimensional (1-D) wave equation on the model output (i.e., wave displacement), to adopt the 1-D wave as a candidate model. However, the uncertainties in initial and boundary conditions, which are composed of the spatiotemporal variables, should influence the numerical simulation (e.g., Fujita et al. [12]; Pettersson et al. [27]). Unlike Gottlieb and Xiu's investigation which was only based on the uncertainty of the model parameter, this study focuses on the effect of uncertainties in the initial and boundary conditions to the wave equation. In theory, the proposed model can take into account the variation and covariance of the wave displacements in time and space. In addition, referring to several studies (e.g., Muscolino et al. [24]; Impollonia and Ricciardi [17]; Nagy and Braatz [25]; Motamed et al. [23]), this study also applies the Monte Carlo simulation method associated with the numerical solution of the wave equation to calculate the statistics of wave displacements, which are regarded as the exact solutions, and compares them with results from the proposed approach. Details of the model development are expressed below.

3.1. Introduction to wave equation

Wave phenomena appear in a wide variety of physical settings in many fields such as: electrodynamics, quantum mechanics, fluid, plasma, atmospheric physics and seismology. One of the most fundamental equations

in applied mathematics and mathematical physics is the wave equation. The 1-D wave equation primarily describes traveling-waves, and is expressed as:

$$\frac{\partial^2 u}{\partial t^2} = c_w^2 \frac{\partial^2 u}{\partial x^2}, \tag{15}$$

where $u(x, t)$ denotes the wave displacement at time t and position x, and the constant c_w is the wave speed.

The numerical solution of the wave equation can be derived by using the explicit finite difference scheme, as shown below:

$$u_{i+1}^{j+1} = 2u_{i+1}^{j} - u_{i+1}^{j-1} + C_r^2(u_{i+2}^{ji} - 2u_{i+1}^{j} + u_i^{jk}),$$

$$C_r = c\frac{\Delta t}{\Delta x}, \tag{16}$$

where Δt and Δx denote the time step and distance increment, respectively; C_r is the Courant number, and j and i are the time and location indicators, namely, $t = j \times \Delta t$ and $x = i \times \Delta x$, respectively. Note that the wave equation requires two initial conditions (ICs), and specifies the initial value and the initial time-derivation of the unknown function as:

$$\text{I.C.} \quad u(x, t = 0) = u_0(x),$$

$$\left.\frac{du}{dt}\right|_{t=0} = g(x), \tag{17}$$

where the functions $u_0(x)$ and $g(x)$ are available. In the case of finding a solution in a finite 1-D domain: $D = \{x \mid X_L \le x \le X_R\}$, the corresponding boundary conditions are required at both ends of the domain as:

$$BC: u(x = 0, t) = u_L(x = X_L, t)$$

$$u(x = L, t) = u_R(x = X_R, t), \tag{18}$$

where the functions $u_L(t)$ and $u_R(t)$ are given. Therefore, at $t = 0$, equation (16) can be rewritten as:

$$u_i^1 = 2u_i^0 - u_i^{-1} + C_r^2(u_{i+1}^0 - 2u_i^0 + u_{i-1}^0) \tag{19}$$

in which u_j^{-1} can be yielded from the initial condition $\left.\frac{du}{dt}\right|_{t=0} = g(x)$. That is,

$$\frac{u_i^1 - u_i^{-1}}{2\Delta t} = g(x) \rightarrow u_i^{-1} = u_i^1 - 2g(x)dt. \tag{20}$$

Substituting equation (19) for equation (18), the wave displacement u_j^1 can be solved as follows:

$$u_i^1 = u_i^0 + g(x)\Delta t + \frac{1}{2}C_r^2(u_{i+1}^0 - 2u_i^0 + u_{i-1}^0). \tag{21}$$

3.2. Derivation of expected value formula for wave equation

According to the model development framework, the explicit numerical solution is regarded as a function of the spatial and temporal variates $u_{i+1}^{j+1} = f(u_{i+1}^j, u_{i+2}^j, u_i^{j+1}, ...)$, and is used to derive the formula for calculating the expected value (mean, standard deviation and coefficient of variance) by equations (1), (4) and (5). Since there are different explicit numerical solutions for $u(x, t)$ at $i = 1$ and $j > 2$, the associated formula for the expected value of the wave displacement should be derived separately.

3.2.1. Formula for mean

At $j = 1$, the mean of the wave displacement $u(x, t)(E[u_{i+1}^1])$ can be derived using equations (2) and (20) as follows:

$$E[u_{i+1}^1] = E\left[u_{i+1}^0 + g(x)\Delta t + \frac{1}{2}C_r^2(u_{i+1}^0 - 2u_{i+1}^0 + u_i^0)\right]$$

$$= E[u_{i+1}^0] + E[g(x)]\Delta t + \frac{1}{2}C_r^2(E[u_{i+2}^0 - 2u_{i+1}^0 + u_i^0]). \tag{22}$$

For $j > 1$, the mean of $u(x = i \times \Delta x, t = j \times \Delta t)$ is obtained by using equations (4) and (16),

$$E[u_{i+1}^{j+1}] = E\{2u_{i+1}^{j} - u_{i+1}^{j-1} + C_r^2(u_{i+2}^{j} - 2u_{i+1}^{j} + u_i^{j})\}$$

$$= 2(1 - C_r^2)E[u_{i+1}^{j}] - E[u_{i+1}^{j-1}] + C_r^2 E[u_{i+2}^{j}] + C_r^2 E[u_i^{j}]. \quad (23)$$

3.2.2. Formula for standard deviation and coefficient of variance

Referring to equation (1), the standard deviation and coefficient of variance is composed of $E[(u_{i+1}^{j+1})^2]$ and $E[u_{i+1}^{j+1}]$. This means that the standard deviation and coefficient of variance can be calculated using equation (1) in the case where $E[(u_{i+1}^{j+1})^2]$ and $E[u_{i+1}^{j+1}]$ are given. Therefore, $E[(u_{i+1}^{j+1})^2]$ should be found in advance. At $j = 1$, $E[(u_{i+1}^{k+1})^2]$ can be formulated from equation (20) as:

$$E[(u_{i+1}^{1})^2] = E\left\{\left[u_{i+1}^{0} + g(x)\Delta t + \frac{1}{2}C_r^2(u_{i+2}^{0} - 2u_{i+1}^{0} + u_i^{0})\right]^2\right\}$$

$$= (1 - 2C_r^2 + C_r^4)E[(u_{i+1}^{0})^2] + E[g(x)^2](\Delta t)^2 + \frac{1}{4}C_r^4\{E[(u_{i+2}^{0})^2] + E[(u_i^{0})^2]\}$$

$$+ (C_r^2 - C_r^4)\{E[u_{i+1}^{0}u_{i+2}^{0}] + E[u_{i+1}^{0}u_i^{0}]\} + 2C_r^2 E[g(x)]\{E[u_{i+2}^{0}] + E[u_i^{0}]\}\Delta t$$

$$+ 2(1 - C_r^2)E[g(x)]E[(u_{i+1}^{0})]\Delta t + 2C_r^4 E[u_{i+2}^{0}u_i^{0}]. \quad (24)$$

Similarly, for $j > 1$, $E[(u_{i+1}^{j+1})^2]$ can be formulated from equation (15):

$$E[(u_{i+1}^{j+1})^2]$$

$$= E\{[2u_{i+1}^{j} - u_{j+1}^{j-1} + C_r^2(u_{i+2}^{j} - 2u_{i+1}^{j} + u_i^{j})]^2\}$$

$$= 4(1 - 2C_r^2 + C_r^4)E[(u_{i+1}^{j})^2] + E[(u_{i+1}^{j-1})^2] + C_r^4\{E[(u_{i+2}^{j})^2] + E[(u_i^{j})^2]\}$$

$$+ 4C_r^2(1 - C_r^2)\{E[u_{i+1}^{j}u_{i+2}^{j}] + E[u_{i+1}^{j}u_i^{j}]\} - 4(1 - C_r^2)E[u_{i+i}^{j}u_{i+1}^{j-1}]$$

$$- 2C_r^2\{E[u_{i+1}^{j-1}u_{i+2}^{j}] + E[u_{i+1}^{j-1}u_i^{j}]\}. \quad (25)$$

Referring to equations (24) and (25), there are five kinds of expected values of the product of the wave displacement at different time steps and positions: $E[u_{i+2}^{j}u_{i}^{j}]$, $E[u_{i+1}^{j}u_{i+2}^{j}]$, $E[u_{i+1}^{j}u_{i}^{j}]$, $E[u_{i+1}^{j-1}u_{i+2}^{j}]$ and $E[u_{i+1}^{j-1}u_{i}^{j}]$ to be calculated by using equation (12). As $E[(u_{i+1}^{j+1})]$ and $E[(u_{i+1}^{j+1})^2]$ are estimated, the mean, standard deviation and coefficient of variance can be obtained using equation (1). Note that the derived formula for the statistics, arrived at by incorporating the expected value operator with the numerical solution of the 1-D wave equation, is named EVO_NS_WE model in this study.

4. Results and Discussion

In the Monte Carlo simulation model, stochastic inputs are generated and then entered into the deterministic models of the underlying physical process to obtain the generated stochastic outputs. Finally, the generated outputs are statistically analyzed to quantify the uncertainty in the outputs (Samani and Solimani [32]). Therefore, in this study, the generated spatiotemporal variates (i.e., wave displacement) for the initial and boundary conditions should be completed based on their statistical properties (i.e., expected values of various orders), which are given in advance. Then, they are imported into the explicit numerical solution of the wave equation (1) to yield the simulation sets of spatiotemporal wave displacement for the entire domain. Thus, the corresponding statistical properties can be calculated from the simulations of initial and boundary conditions. Eventually, the resulting statistics, i.e., the mean, standard deviation and coefficient of variance of the wave displacements from the proposed EVO_NS_WE model, are compared with those obtained by the Monte Carlo simulation method integrated with the explicit numerical solution of the wave equation (named MCS_NS_WE model), in the case of the mean and coefficient of variance of the initial and boundary conditions being given.

4.1. Simulation of initial and boundary conditions

In general, most numerical methods developed for hyperbolic equations

are explicit but subject to the well-known Courant-Friedrichs-Lewy (CFL) condition (Courant et al. [3]). That is to say, Courant number $C_r = c_w\, dt/dx$ (the stability condition) should be equal to or less than 1.0 in a hyperbolic equation. Therefore, in order to derive the explicit numerical solution which can converge in time, this study assigns the increments of time step (i.e., Δt and Δt) as 10sec and 100cm, respectively, with a specified wave speed $(c_w = 10\text{cm/s})$, so that the courant number C_r is exactly equal to 1.0 in the specific domain.

Since this study focuses on the effect of uncertainties in the initial and boundary conditions on the computation of the wave displacement $u(x, t)$ in the domain, the statistical properties, the means of spatiotemporal variables for the initial and boundary conditions, are given in Figure 1, and the coefficients of variance are assigned as 0.7 (initial conditions) and 0.65 (boundary conditions). Also, their behavior can be described by the normal probability distribution. Moreover, in reality, the wave displacement at various positions and time steps should be highly correlated spatiotemporal variables so that their correlation coefficients are assumed as one in this study. Thus, this study employs the multivariate Monte Carlo simulation model for the non-normal correlated variates, as developed by Wu et al. [40], to generate wave displacements as the initial and boundary conditions.

In the MCS_NS_WE model, the simulation number of initial and boundary conditions should be determined in advance. Therefore, in this study, an essential assessment for the number of generating initial and boundary conditions is carried out by varying the simulation number from 50 to 3000 sets in order to compute the statistics of wave displacements at the desired time steps and grids. Figure 2 shows the mean value of the wave displacements for $t = 20$ sec, 50sec and 80sec. It can be seen that the mean of the wave displacements gradually varies with the simulation number. For illustration, at $x = 200$ cm and $t = 20$ sec, the mean declines from 40cm to 21cm with the simulation number varying from 50 sets to 3000 sets; however, the mean at $t = 50$ sec smoothly rises from -0.5cm to 10cm and the ones at $t = 50$ sec stay in a constant of 21cm when the simulation number is

over 1000 sets. Moreover, for $x = 800$ cm, there is oppositive change in the mean at $t = 20$ sec and 50sec. To sum up the above results, it can be said that the number of simulated initial and boundary conditions exceeding 1000 sets would be suitable for the calculation of average wave displacements using the MCS_MS_WE model.

Figure 3 indicates the change in the variance of wave displacements with varying simulation number from 50 sets to 3000 sets. It is observed that the varying trend of the variance of the wave displacement resembles that of the mean, but the variance more rapidly changes with the simulation number than the mean does. In detail, the variance first rises from 50 sets to 200 sets, and then declines from 200 sets to 1000 sets. Finally, the variance remains a constant when the simulation number exceeds 1000 sets. For example, at $x = 100$ cm and $t = 80$ sec, the variance increases from 140cm^2 to 153cm^2 as the simulation number varies from 50 sets to 1000 sets and decreases to 120cm^2 for simulation number over 1000 sets. Therefore, when the simulation number is equal to or more than 1000 sets, the stable results from the variance can be obtained for different time steps and locations.

To sum up the results from the mean and variance with various simulation numbers of initial and boundary conditions, the 1000 sets of simulated initial and boundary conditions are adopted in the MCS_NS_WE model and the resulting statistics of wave displacements are regarded as the exact solutions for the demonstration of the proposed EVO_NS_WE model.

4.2. Calculation of approximation of statistical properties

In this subsection, the statistical properties of wave displacement are calculated by the proposed EVO_NS_WE models and MCS_NS_WE model based on the given mean and coefficient of variance (CV) for the initial and boundary conditions, respectively. Note that since the wave displacement belongs to the non-positive spatiotemporal variable, the corresponding change in time would be negative; therefore, the CV is adopted to compare the change of the wave displacement in time calculated by the proposed EVO_NS_WE model and the MCS_NS_WE model, respectively, due to the standard deviation being positive.

(1) MCS_NS_WE model

1000 simulations of initial and boundary conditions are accomplished using the multivariate Monte Carlo simulation method and then imported into the numerical solution of the wave equation (16). The resulting 1000 simulations of the wave displacement at each time step and position are obtained and the associated mean and CV are calculated, as shown in Figures 4 and 5; thus, the mean and CV at different times and positions are known. Specifically, the mean (61cm) and CV (-21.51) at $(x = 500\,\text{cm},\ t = 0\,\text{sec})$ and $(x = 200\,\text{cm},\ t = 90\,\text{sec})$ are at their maximum, respectively.

(2) EVO_NS_WE model

According to the proposed framework for modeling the uncertainty analysis, the mean value of the wave displacement could be calculated in advance by the EVO_NS_WE model. Figure 6 shows the approximations of the mean values; they are similar to the results from the MCS_NS_WE model where the resulting mean at $t = 0$ sec is at its maximum (60cm). As in estimating the CV, the information on the spatiotemporal semivariogram for the expected value of the product of variables with respect to the different time steps and positions should be required. This study adopts the estimated mean values of wave displacements in the entire domain to determine the best-fit spatiotemporal semivariogram model and calibrates the associated parameters, as shown in Table 2. This table shows that the Gaussian model is the best-fit model in time and space, respectively, as well as the associated optimal parameters. Therefore, through equation (8), the coefficients k_1, k_2 and k_3 are 0.0012, 0.0 and 0.798, respectively. Eventually, the expected value of product of the wave displacement could be obtained and utilized in the calculation of the approximation of CV, as shown in Figure 7. In view of Figure 5, the CV is at its maximum (approximately 25.5) for $x = 800$ cm and $t = 90$ sec.

4.3. Comparison of EVO_NS_WE and MCS_NS_WE models

This subsection compares the proposed EVO_NS_WE model and MCS model in the computation of the mean, standard deviation and CV of

the spatiotemporal variates at different time steps and positions. The comparisons are made by calculating and evaluating the performance indices.

4.3.1. Performance indices

To compare the mean and coefficient of variance of the wave displacement and flow depth computed by the proposed EVO_NS_WE model with those of the MCS_NS_WE model, two model performance indices are employed: the root mean square error (RMSE) and model reliability index (KS) (Leggett and Williams [20]). RMSE and KG are defined as:

1. Root mean square error (RMSE):

$$RMSE = \frac{1}{N_t}\sqrt{\sum_{i=1}^{N_t}[\phi_{\text{model}}(x,\ t) - \phi_{MCS}(x,\ t)]^2},$$

$$t = k \times \Delta t;\ x = (1,\ 2,\ ...,\ N_g) \times \Delta x. \tag{26}$$

2. Model reliability index (Leggett and Williams [20]):

$$KS = \exp\left\{\sqrt{\frac{1}{N_t}\sum_{k=1}^{N_t}\left[\log\left(\frac{\phi_{\text{model}}(x,\ t)}{\phi_{\text{MCS}}(x,\ t)}\right)\right]^2}\right\},$$

$$t = k \times \Delta t;\ x = (1,\ 2,\ \cdots N_g) \times \Delta x, \tag{27}$$

where $\phi_{\text{model}}(x,\ t)$ and $\phi_{\text{MCS}}(x,\ t)$ denote the statistics of spatiotemporal variates obtained by the proposed EVO_NS_WE model and MCS_NS_WE model; and N_g and N_t denote the number of grids and total time period in the domain used. Note that a small RMSE indicates that the estimated mean, standard deviation and coefficient of variance calculated by the proposed model are closer to those using the MCS_NS_WE model. Moreover, KS, approaching 1.0 implies that the variation in the temporal trend of the statistical properties calculated by the proposed model resembles those obtained by the MCS_NS_WE model.

4.3.2. Comparison of mean value

To evaluate the differences in the mean and variance of the wave displacement estimated by the EVO_NS_WE and MCS_NS_WE models, a graphical comparison is made with respect to time where $x = 100 \sim 900\,\text{cm}$, excluding boundaries, $x = 0\,\text{cm}$ and $x = 1000\,\text{cm}$, as shown in Figure 8. Furthermore, the model performance indices for different positions are calculated, as shown in Figure 9. As far as the mean is concerned, the mean values estimated by the proposed EVO_NS_WE model are significantly close to those obtained by the MCS_NS_WE model. The root mean square error for the mean value RMSE is equal to 0, and the corresponding model reliability index KS approaches 1.0. This implies that the estimated mean values of wave displacement by the proposed EVO_NS_WE model, with respect to time and space, match those by the MCS model very well. It can be said that the proposed EVO_NS_WE model agrees well with the MCS_NS_WE model in terms of the mean value.

4.3.3. Comparison of coefficient of variance (CV)

Figure 10 shows the visual comparison of the CV value of the wave displacement obtained by the proposed EVO_NS_WE model and the MCS_NS_WE model at particular positions. It is known that the fitness of the CV estimated by the proposed model compared to that obtained by the MCS_NS_WE model is slightly poorer than that of the mean. However, the varying trends of CV with time estimated by the proposed EVO_NS_WE model and MCS_NS_WE model are comparable. For example, except for $x = 100\,\text{cm}$ and $x = 900\,\text{cm}$, in which the CV increases with time, the CV resulting from the MCS model gradually rises before $t = 70\,\text{sec}$ or 80sec. The CV then rapidly decreases at $t = 70\,\text{sec}$ or 80sec, and then increases again. Similar results could be found for the CV estimations by the proposed model.

Referring to Figure 11, most of the RMSE values are between 0.2 and 1 (on average 0.6), except at $x = 800\,\text{cm}$, where the RMSE is approximately

1.2 due to a large CV value (20.1) associated with the maximum difference from the estimation given by the MCS_NS_WE model. Moreover, the model reliability index KS for the CV ranges from 1.0 to 1.5, and the average approximates 1.43. This indicates a slight difference between the proposed model and MCS_NS_WE model in the estimations of the CV at different positions. This difference is possibly attributed to the product of the spatiotemporal variables at various time steps and positions. Nevertheless, the proposed EVO_NS_WE model could continually capture the varying trend of the CV value with time. Consequently, the proposed EVO_NS_WE model could provide approximations of the CV with acceptable differences as compared with those using the MCS_NS_WE model.

4.4. Assessment of uncertainty in the initial and boundary conditions

In general, uncertainty can be described based on statistical properties, especially for the coefficient of variance (CV), which accounts for the dispersion from the expected value. Since the proposed EVO_NS_WE models can effectively provide the approximations of the mean, standard deviation and CV, the effects of the variation of the initial and boundary conditions on spatiotemporal variables (model output) can be evaluated via the proposed models.

Figure 12 shows the average varying ratio of the CV for the wave displacement $u(x, t)$ based on an estimated CV by the MCS_NS_WE model, excluding the initial time $t = 0\,\text{sec}$ and boundaries $x = 0\,\text{cm}$ and $x = 1000\,\text{cm}$ under the consideration of the variation of CV for initial conditions $(\text{IC1: } u(x, t = 0)$ and $\text{IC2: } du(x, t)/dt|_{t=0})$ and boundary conditions $(\text{BC1: } u(x = 0, t)$ and $\text{BC2: } u(x = Ll, t))$. It can be shown that the average varying ratio of the CV for the wave displacement $u(x, t = 0 \sim T)$ at different positions increases with the varying ratio of the CV of the initial and boundary conditions. For example, the wave displacement has a maximum average varying ratio of the CV (from approximately 0.5 to 0.9) since the varying ratio of the CV for IC1 increases

from 0.1 to 0.5, whereas the wave displacement approximates a constant 0.5 in the case of IC2 being from 0.1 to 0.5. In addition, the resulting average ratios of the CV for the wave displacement from boundary conditions BC1 and BC2 are located between those from IC1 and IC2. Specifically, as for $100\text{cm} < x < 500\text{cm}$, the average varying ratios of CV for the wave displacement attributed to BC1 are greater than those due to BC2. Nevertheless, contrary results can be found for $500\text{cm} < x < 9000\text{cm}$. It can be also seen that for $x = 100\,\text{cm}$ and $x = 900\,\text{cm}$, the average varying ratios of the CV for $u(x,\, t = 0 \sim T)$ are significantly classified into two parts: one is IC1 and BC2 (about 0.4) and the other group is IC2 and BC1.

5. Conclusions

This study proposed an alternative framework of modeling uncertainty analysis to calculate the approximations of statistical properties of spatiotemporal variables for evaluating the effect of initial and boundary conditions on the output of numerical models. This is accomplished by incorporating the expected value operator into the explicit numerical solutions of the corresponding governing equations. To take into account the correlation of variables in time and space, spatiotemporal semivariogram models are employed in this study. The 1-D wave equation is adopted in the model development and demonstration. Results from the model validation show that the proposed models can directly and effectively provide approximations of the mean value of the wave displacement that well match the results from the Monte Carlo simulation model and approximations of the coefficient of variance with acceptable differences from those obtained using the Monte Carlo simulation model. Also, it is evident that the variation of the boundary condition leads to more uncertainties in the wave displacement than found in the initial boundary.

Although the proposed model can effectively produce the mean and coefficient of variance of wave displacements by means of integrating the expected value operator with the explicit numerical solution of the wave

equations, it only takes into account the uncertainties in the initial and boundary conditions. However, several investigations indicated that the variation in the wave speed should affect the estimation of the wave displacements (e.g., Gottlieb and Xiu [14]; Tang and Zhou [36]; Motamed et al. [23]). Therefore, future work should be undertaken concerning the uncertainties in the wave speed and initial as well as boundary conditions to derive the expectation value formula for calculating the statistics of wave displacements. Eventually, it is expected that the presented stochastic modeling framework could be applied in other 1-D and 2-D numerical models associated with linear and nonlinear governing equations to evaluate stochastic properties of the model outputs and to provide corresponding probabilistic information under consideration of uncertainties in initial and boundary conditions.

Table 1. Commonly used theoretical semivariogram models and their parameters

Model	$\gamma(h)$	Range of h
1. Spherical model	$c\left[\frac{3h}{2a}-\frac{1}{2}\left(\frac{h}{a}\right)^3\right]$	$0 \leqq h \leqq a$
	c	$h > a$
2. Exponential model	$c\left[1-\exp\left(\frac{-h}{a}\right)\right]$	$h \geqq 0$
3. Gaussian model	$c\left[1-\exp\left(\frac{-h^2}{a^2}\right)\right]$	$h \geqq 0$
4. Power model	ch^a	$h \geqq 0;\ 0 < a \leqq 2$
5. Nugget model	0	$h = 0$
	c	$h \geqq 0$
6. Linear model	Ch	$h \geqq 0$
7. Linear-with-sill model	$c\left(\frac{h}{a}\right)$	$0 \leqq h \leqq a$
	c	$h > a$

8. Circular model	$c\left[\frac{2h}{\pi a}\sqrt{1-\left(\frac{h}{a}\right)^2}+\frac{2}{\pi}\arcsin\frac{h}{a}\right]$	$0 \leqq h \leqq a$
	c	$h > a$
9. Pentaspherical model	$c\left[\frac{15h}{8a}-\frac{5}{4}\left(\frac{h}{a}\right)^3+\frac{3}{8}\left(\frac{h}{a}\right)^5\right]$	$0 \leqq h \leqq a$
	c	$h > a$
10. Logarithmic model	0	$h = 0$
	$c[\log(h+a)]$	$h > 0$
11. Periodic model	$c\left[1-\cos\left(\frac{2\pi h}{a}\right)\right]$	$h \geqq 0$

Note that c and a denote the sill and influence range; and h denotes distance (Davis [4]).

Table 2. Types of parameters of the best-fit spatiotemporal semivariogram models for proposed EVO_NS_WE model

Semivariogram	Best-fit model	Parameter	
		a_0	c_0
Spatial	Gaussian	167.5	101.2
Temporal	Gaussian	52.6	1131.6

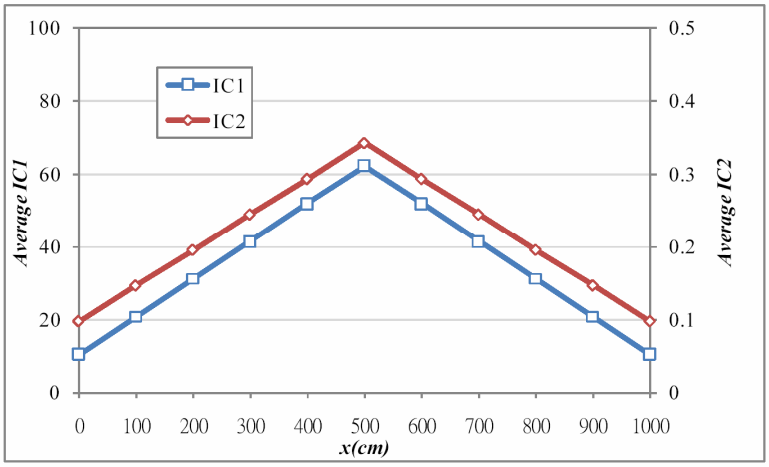

(1) Initial conditions $\mathrm{IC1} = u(x,\, t = 0)$ and $\mathrm{IC2} = du\,(x,\, t)/dt\,|_{\,t=0}$

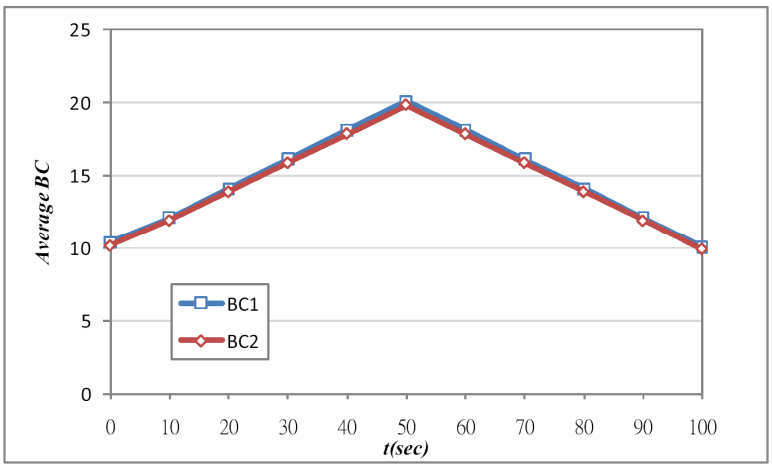

(2) Boundary conditions $\mathrm{BC1} = u(x = 0,\, t)$ and $\mathrm{BC2} = u(x = L,\, t)$

Figure 1. Assumption of the mean value of wave displacement for initial and boundary conditions $(L = \text{distance})$.

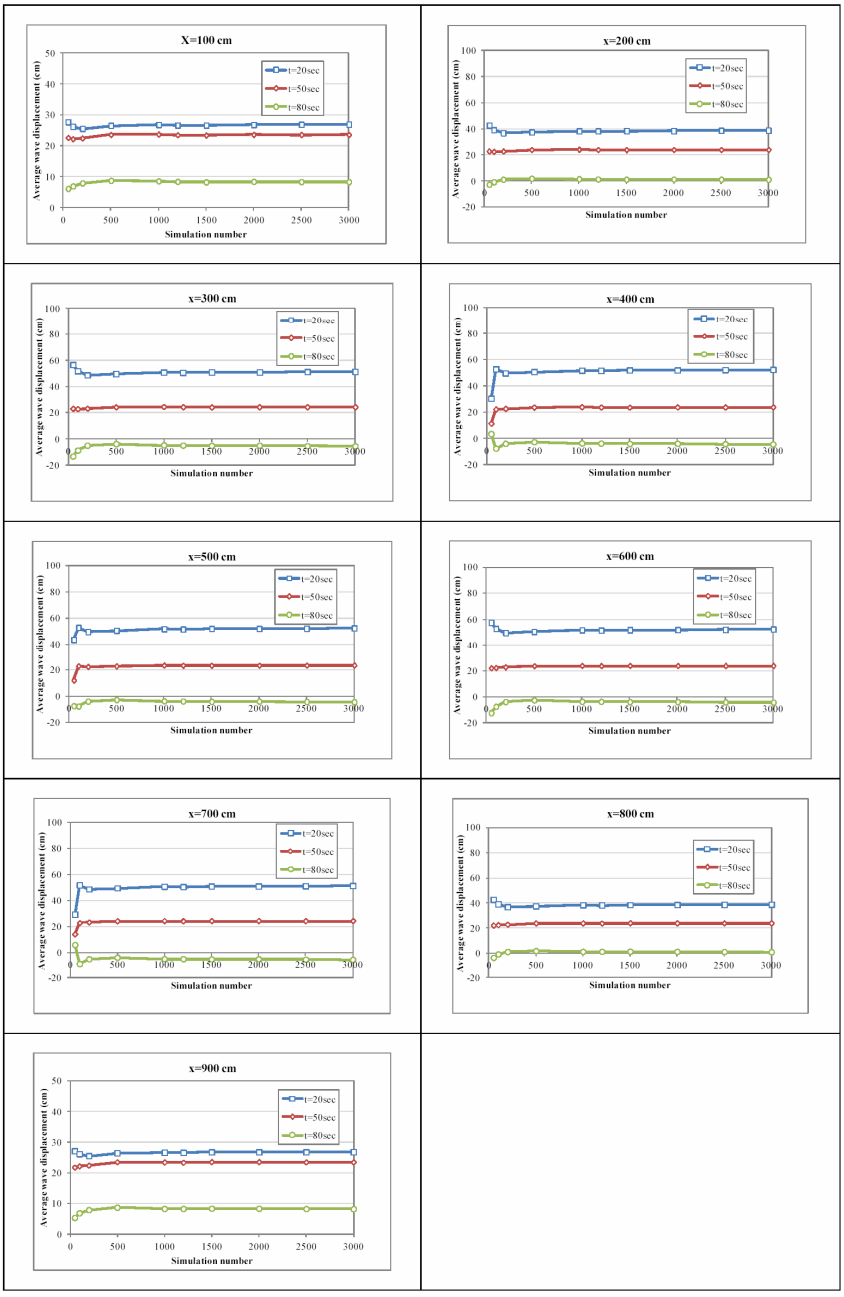

Figure 2. Summary for varying average wave displacement with the simulation number of initial and boundary conditions for different locations.

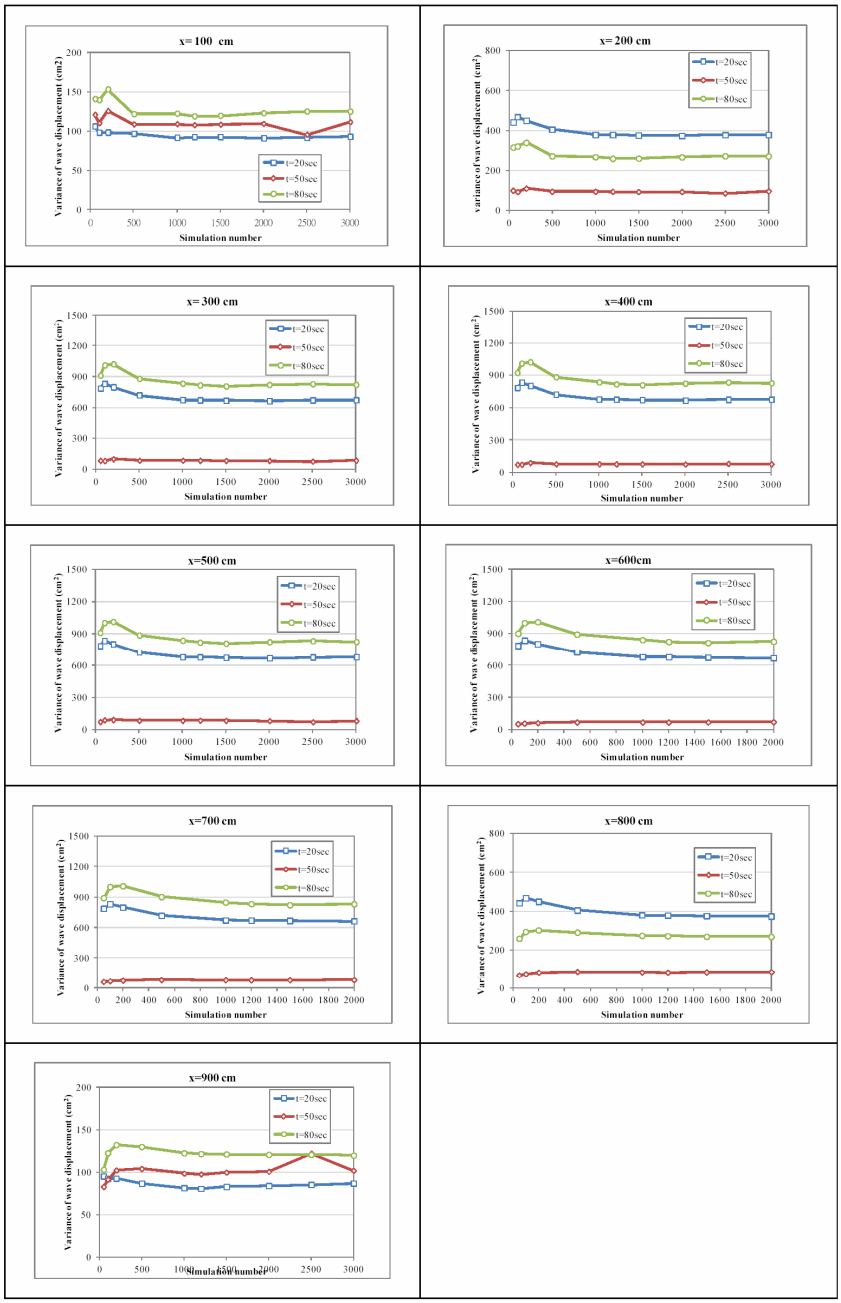

Figure 3. Summary for variances of wave displacements with the simulation number of initial and boundary conditions for different locations.

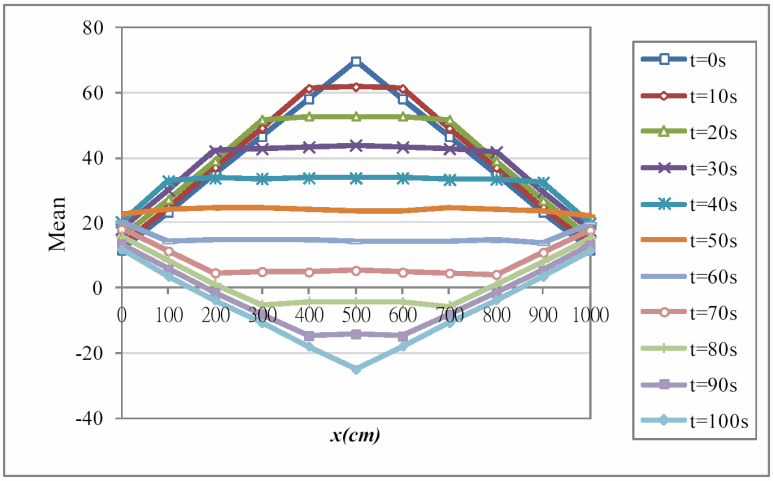

Figure 4. Mean values of wave displacements estimated by MCS_NS_WE model.

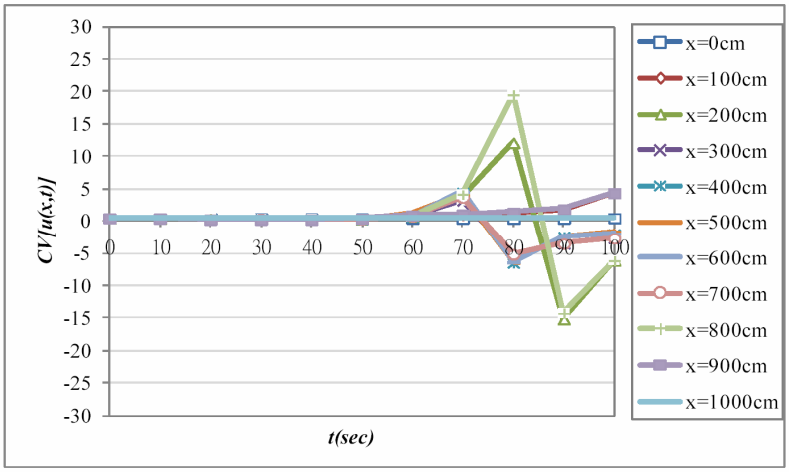

Figure 5. Coefficient of variance (CV) estimated by MCS_NS_WE mode.

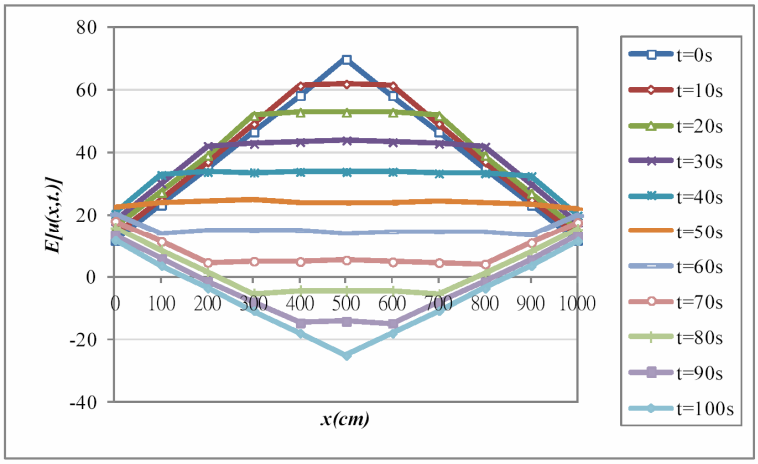

Figure 6. Mean values of wave displacements estimated by EVO_NS_WE model.

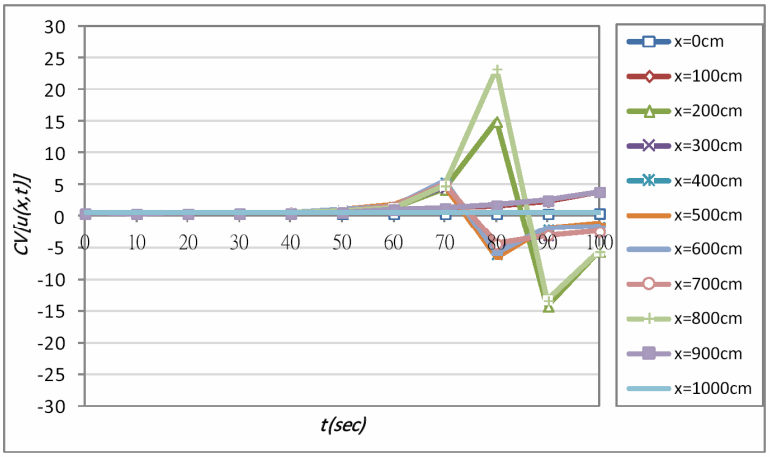

Figure 7. Coefficient of variance (CV) estimated by EVO_NS_WE mode.

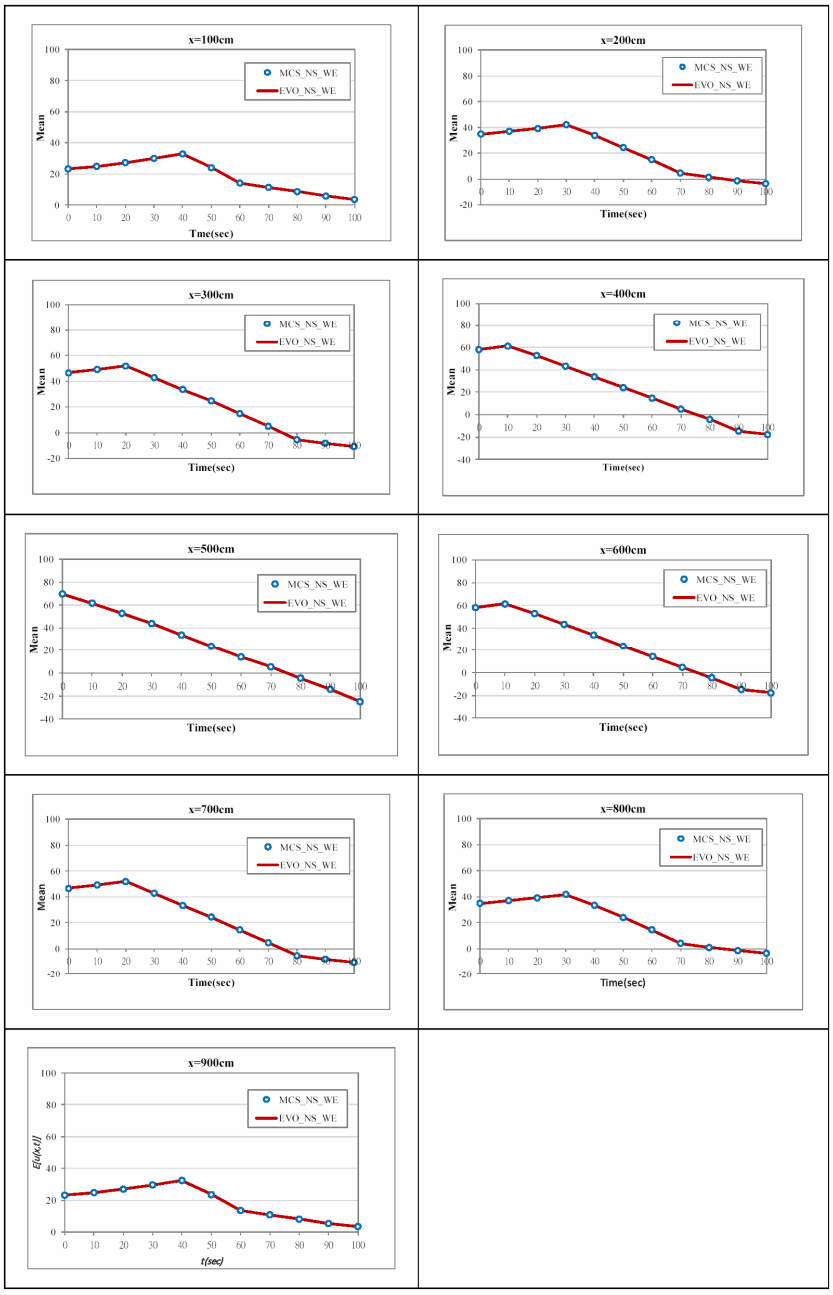

Figure 8. Comparison of the mean values of wave displacement calculated by MCS_NS_WE and EVO_NS_WE models.

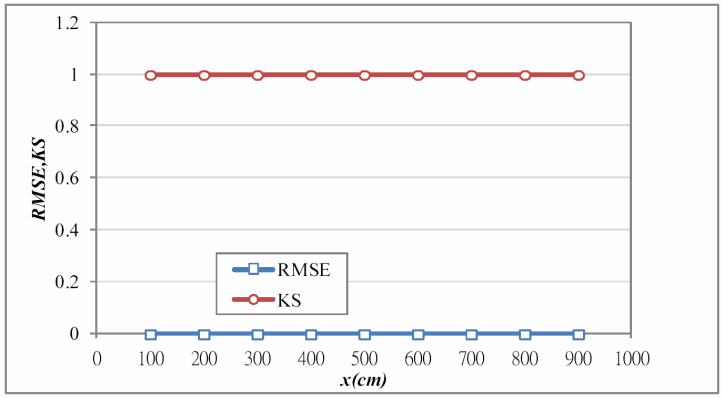

Figure 9. Performance indices for mean of wave displacement calculated by proposed EVO_NS_WE model.

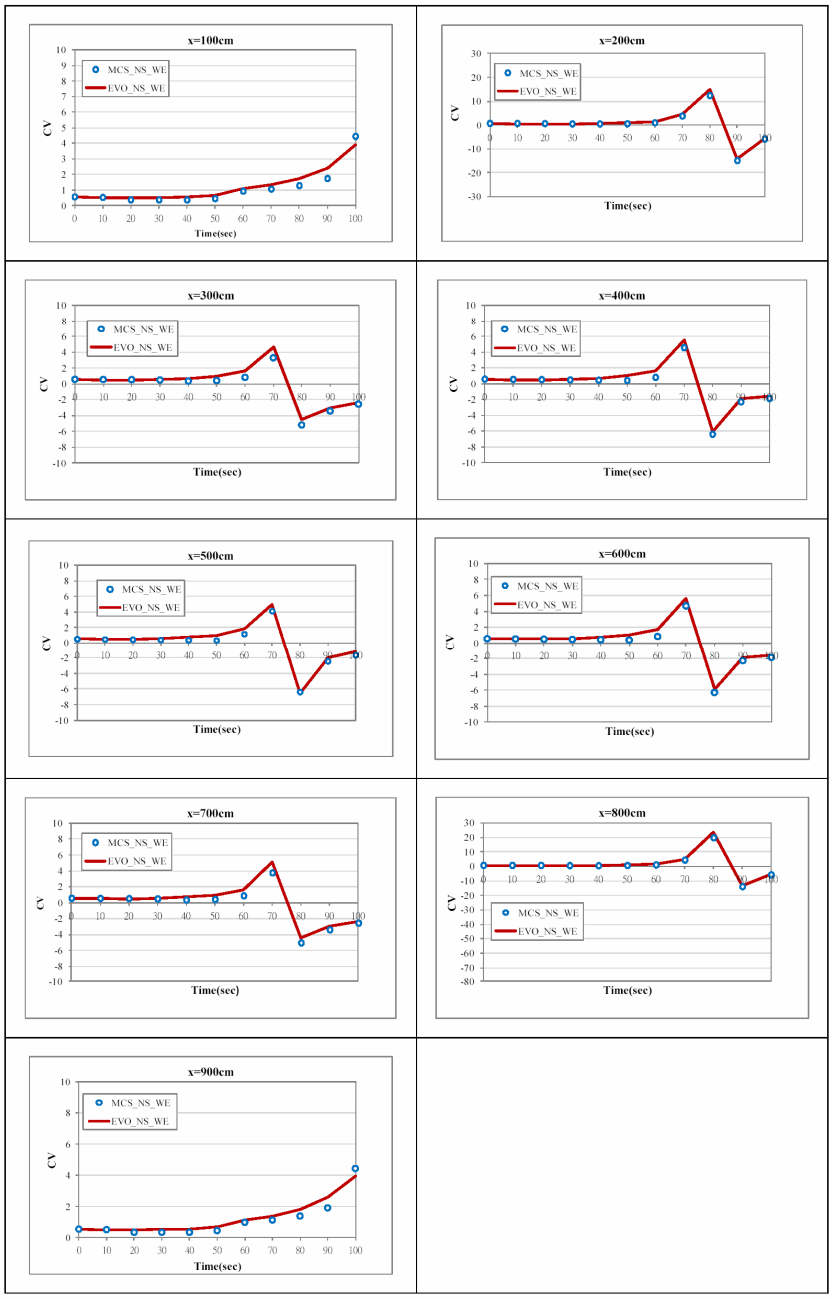

Figure 10. Comparison of the coefficient of variance (CV) of wave displacement calculated by MCS_NS_WE and EVO_NS_WE.

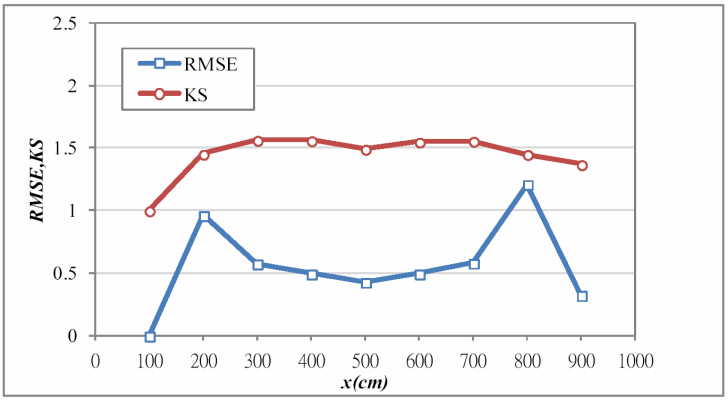

Figure 11. Performance indices for coefficient of variance (CV) of wave displacement calculated by proposed EVO_NS_WE model.

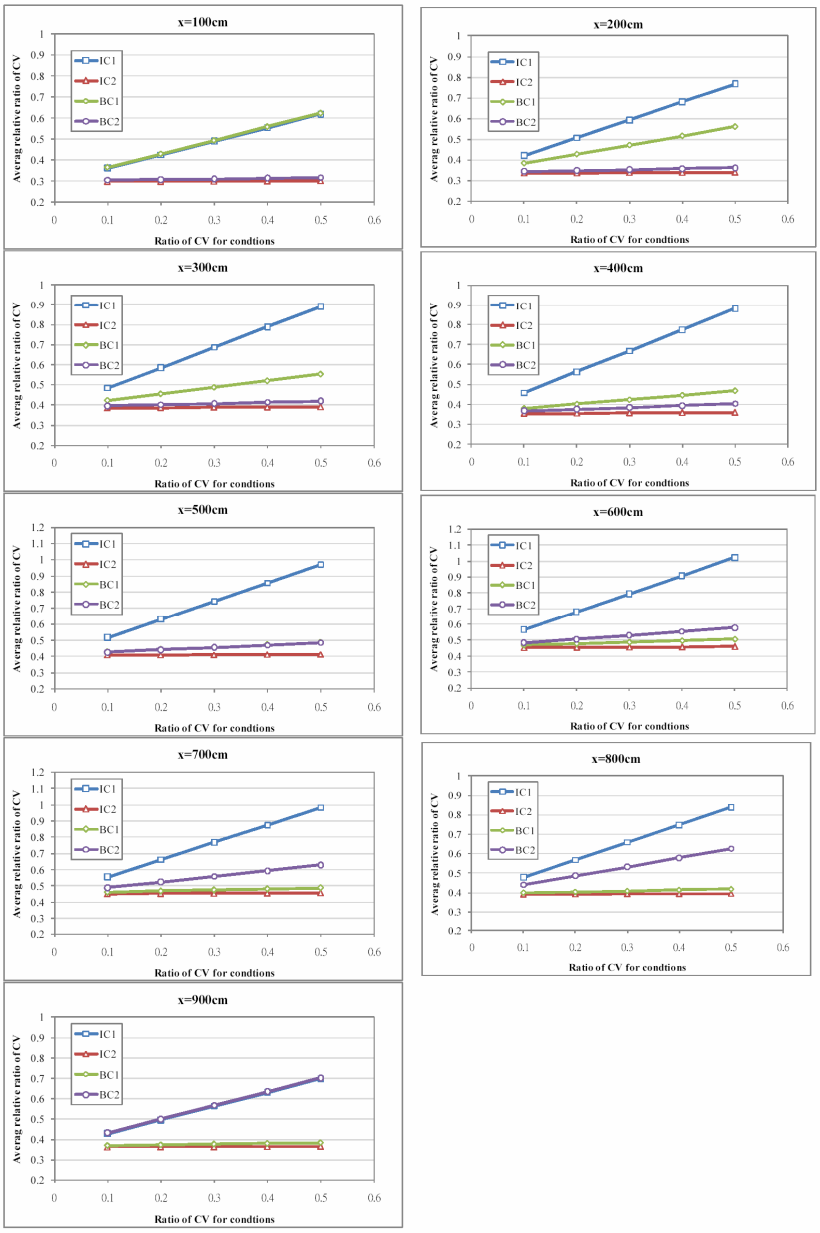

Figure 12. Average relative ratio of CV for wave displacement based on varying ration of CV for conditions $(\text{IC1} = u(x, t = 0);\ \text{IC2} = du(x, t)/dt|_{t=0};$ and $\text{BC2} = u(x = L, t))$ using EVO_NS_WE model.

References

[1] C. Agut, J. Diaz and A. Ezzizni, High-order schemes combining the modified equation approach and discontinuous Galerkin approximation for the wave equation, Commun. Comput. Physics 11(2) (2012), 691-708.

[2] F. Collard and M. Juillard, Accuracy of stochastic perturbation methods: the case of asset pricing models, J. Econom. Dynam. Control 25 (2001), 979-999.

[3] R. Courant, K. O. Friedrichs and H. Lewy, Uber die partiellen differenzen-gleichungen der mathematisches physik, Math. Ann. 100 (1928), 32-74.

[4] J. C. Davis, Statistics and Data Analysis in Geology, John Wiley & Sons, New York, 1973, pp. 239-248, 383-405.

[5] L. De Cesare, D. E. Mayers and D. Posa, Product-sum covariance for space-time modeling: an environmental application, Environmetrics 12 (2001), 11-23.

[6] L. De Cesare, D. E. Mayers and D. Posa, FORTRAN programs or space-time modeling, Comput. Geosci. 28 (2002), 205-212.

[7] M. D. Dettinger and J. L. Wilson, First-order analysis of uncertainty in numerical models of groundwater Part 1. Mathematical development, Water Resources Research 17(1) (1981), 149-161.

[8] F. A. DiazDelao and S. Adhikari, Coupling polynomial chaos expansions with Gaussian process emulators: an introduction, Proceedings of the IMAC-XXVII, Orlando, Florida, USA, 2009.

[9] R. Dimitrakopoulos and X. Luo, Spatiotemporal modeling: covariance and ordinary kriging system, Geostatistics for the Next Century, Kluwer Academic Publishers, Dordrecht, 1993, pp. 88-93.

[10] I. Elishakoff, Y. J. Ren and M. Shinozuka, Improved finite element method for stochastic problems, Chaos Solitons Fractals 5(5) (1995), 846-883.

[11] G. Falsone and N. Impollonia, A new approach for the stochastic analysis of finite element model structure with uncertain parameters, Comput. Methods Appl. Mech. Engrg. 191(44) (2002), 5067-5085.

[12] T. Fujita, D. J. Stensrud and D. C. Dowell, Surface data assimilation using an ensemble Kalman filter approach with initial condition and model physics uncertainties, Monthly Weather Review 135 (2006), 1846-1868.

[13] T. M. Gneiting, G. Genton and P. Guttorp, Geostatistical Space-time Model, Stationarity, Separability and Full Symmetry, University of Washington, 2005.

[14] D. Gottlieb and D. Xiu, Galerkin method for wave equations with uncertain coefficients, Commun. Comput. Physics 3(2) (2008), 505-518.

[15] M. Gunzburger, Numerical method for stochastic partial differential equations and their control, London Mathematical Society Durham Symposium, Durham, UK, 2008.

[16] J. E. Hurtado and A. H. Barbat, Monte Carlo techniques in computational stochastic mechanics, Arch. Comput. Methods Engrg. 5(1) (1998), 3-29.

[17] N. Impollonia and G. Ricciardi, Explicit solution in the stochastic dynamics of structure system, Probabilistic Engineering Mechanics 21(2) (2006), 171-181.

[18] M. L. Kavvas and R. S. Govindaraju, Stochastic overland flows-Part 1: Physics-based evolutionary probability distributions, Stoch. Environ. Res. Risk Assess. 5 (1991), 89-104.

[19] Y. H. Kwak and L. Ingall, Exploring Monte Carlo simulation applications for project management, Risk Management 9 (2007), 44-57.

[20] R. W. Leggett and L. R. Williams, A reliability index for models, Ecological Modelling 13 (1981), 303-312.

[21] J. Lin, Analytical approach to the sine-Gordon equation using homotopy perturbation method, Int. J. Contemp. Math. Sci. 4(5) (2009), 225-231.

[22] S. Maskey, Modelling uncertainty in flood forecasting systems, Ph.D. Thesis, A. A. Balkema Publisher, The Netherlands, 2004.

[23] M. Motamed, F. Nobile and R. Tempone, A stochastic collocation method for the second order wave equation with a discontinuous random speed, Numer. Math. 123(3) (2013), 493-536.

[24] G. Muscolino, G. Ricciardi and N. Impollonia, Improved dynamic analysis of structures with mechanical uncertainties under deterministic input, Probabilistic Engineering Mechanics 15(2) (2000), 199-212.

[25] Z. K. Nagy and R. D. Braatz, Distributional uncertainty analysis using power series polynomial chaos expansions, J. Process Control 17 (2007), 229-240.

[26] M. Papadrakakis and V. Papadopoulos, Robust and efficient method for stochastic finite element analysis using Monte Carlo simulation, Computer Methods in Applied Mechanics and Engineering 134(3) (1996), 325-340.

[27] P. Pettersson, G. Iaccarino and J. Nordström, Numerical analysis of the Burgers' equation in the presence of uncertainty, J. Comput. Phys. 228(22) (2009), 8394-8412.

[28] R. Pulch, Polynomial chaos for linear differential algebraic equations with random parameters, Int. J. Uncertainty Quantification 1(3) (2011), 223-240.

[29] R. Pulch, Polynomial chaos for boundary value problems of dynamical systems, Appl. Numer. Math. 62(10) (2012), 1477-1490.

[30] D. L. Roberts and M. S. Selim, Comparative study of six explicit and two implicit finite difference scheme for solving one-dimensional parabolic partial differential equations, Internet J. Numer. Methods. Engrg, 20 (1984), 817-844.

[31] I. Rodriguez-Iturbe and J. Mejia, The design of rainfall networks in time and space, Water Resources Research 10 (1974), 713-728.

[32] J. M. V. Samani and A. Solimani, Uncertainty analysis of routed outflow in rockfill dams, J. Agriculture Science and Technology 10 (2008), 55-66.

[33] W. A. Scharffenberg and M. L. Kavvas, Uncertainty in flood wave routing in a lateral-inflow-dominated stream, J. Hydrologic Engineering 16(2) (2011), 165-175.

[34] C. Singh and X. L. Kim, Power system adequacy and security calculation using Monte Carlo simulation incorporating intelligent system methodology, 9th International Conference on Probabilistic Methods Applied to Power Systems KTH, Stockholm, Sweden, 2006.

[35] Q. Su and K. Strunz, Stochastic-chaos-based average model of twelve-pulse diode rectifier for aircraft application, 2006 IEEE COMPEL Workshop, NY, 2006, pp. 64-66.

[36] T. Tang and T. Zhou, Convergence analysis for stochastic collocation methods to scalar hyperbolic equations with a random wave speed, Commun. Comput. Physics 8 (2010), 226-248.

[37] Y. K. Tung and L. W. Mays, Risk model for flood levee design, Water Resources Research 17(4) (1981), 833-841.

[38] Y. K. Tung and B. C. Yen, Hydrosystems Engineering Uncertainty Analysis, McGraw-Hill Companies, New York, 2008.

[39] S. J. Wang and K. C. Hsu, The application of the first-order second-moment method to analyze poroelastic problems in heterogeneous porous media, J. Hydrology 369 (2009), 209-221.

[40] S. J. Wu, Y. K. Tung and J. C. Yang, Stochastic generation of hourly rainstorm events, Stoch. Environ. Res. Risk Assess. 21(2) (2006), 195-212.

[41] S. J. Wu, H. C. Lien and C. H. Chang, Calibration of conceptual rainfall-runoff model using genetic algorithm integrated with runoff estimation sensitivity to parameters, J. Hydroinformatics, 2011. doi:10.2166/hydro.2011.010.

[42] D. Xiu and G. E. Karniadakis, The Wiener-Askey polynomial chaos for stochastic differential equations, SIAM J. Sci. Comput. 24(2) (2002), 619-644.

[43] D. Xiu and G. E. Karniadakis, Modeling uncertainty in flow simulation via generalized polynomial chaos, J. Comput. Phys. 187(1) (2003), 137-167.

[44] F. Yamazaki, M. Shinozuka and G. Dasgupta, Neumann expansion for stochastic finite element analysis, J. Engineering Mechanics 144 (1988), 1335-1355.

[45] D. Zeitoun and C. Braester, A Neumann expansion approach to flow through heterogeneous formations, Stoch. Environ. Res. Risk Assess. 5(3) (1991), 207-226.

[46] T. Zhou and T. Tang, Galerkin methods for stochastic hyperbolic problems using bi-orthogonal polynomials, J. Science Communication 51 (2012), 274-292.

[47] T. Zhu, J. D. Zhang and S. N. Atluri, A meshless local boundary integral equation (LBIE) method for solving nonlinear problems, Comput. Mech. 22 (1998), 174-186.